17th World Conference on Earthquake Engineering, 17WCEE
Sendai, Japan - September 13th to 18th 2020

DEVELOPMENT OF MULTIPLE ROCKING COLUMN STRUCTUAL SYSTEM

P. Xiang [(1)], R.H. Xie [(2)], Z.F. Li [(3)], L.J. Jia [(4)]

[(1)] *Associate Professor, College of Civil Engineering, Tongji University, Shanghai, China, p.xiang@tongji.edu.cn*
[(2)] *Graduate Student, College of Civil Engineering, Tongji University, Shanghai, China, 1732514@tongji.edu.cn*
[(3)] *Graduate Student, College of Civil Engineering, Tongji University, Shanghai, China, 1732566@tongji.edu.cn*
[(4)] *Associate Professor, College of Civil Engineering, Tongji University, Shanghai, China, lj_jia@tongji.edu.cn*

Abstract

Traditional wooden structures have superior seismic performance, while its mechanism is still open to discussion. Studies on the mortise-tenon joints and the Dou-Gong brackets showed that these joints play an important role in dissipating seismic energy and improving the seismic performance of the wooden structures. It was also found that the column rocking behavior in the traditional structures has a significant impact on their seismic responses. The static and dynamic features of the column rocking behavior have been extensively discussed and clarified, which can be applied to developing new structural systems.

Currently, rocking columns are mainly used as piers in bridge structures but rarely adopted in building structures. A multiple rocking column structural system is proposed in this study. In this system, the beams are continuous, and the top and bottom column endplates can uplift under strong earthquakes. Through this detail, the frame can rock at each story, which is different from base rocking structural systems. Base rocking frames or base rocking walls are reported to have significant high mode effects for high-rise structures, which can lead to large internal forces. With the consideration of higher mode effects, the design force demand of the base rocking systems increases dramatically and the economic viability of the systems is limited. This problem can be solved in the newly proposed multiple rocking column system comprising more rocking interfaces along the structural height.

In order to investigate the seismic performance of the proposed rocking column system, both theoretical and experimental studies are conducted. An analytical model is established and the corresponding equation of motion is obtained by the Lagrange equation. Comparing the equations of a single-story rocking column system and a conventional frame system, it can be found that the former system has larger inter-story drift, but smaller inter-story shear force and secant stiffness in some cases. Four types of structural models are tested on the shaking table, including a single-story rocking column system, a single-story conventional frame system, a multi-story rocking column system and a multi-story conventional frame system. The rocking column system models are designed to be able to easily switch into conventional frame systems. Shear keys are used in the rocking column systems to prevent the sliding between the column end plates and the beam flanges. Test results show that the internal forces as well as the dominant frequencies of the structures could be reduced by the rocking motion. In addtion, the distribution of inter-story drifts is changed due to the exsistence of rocking columns.

Keywords: rocking column, multiple rocking, small shaking table test, seismic performance.

1. Introduction

Traditional wooden structures have superior seismic performance which enables them to survive from severe earthquakes. These structures were usually built based on limited engineering practice. To figure out the mechanism, researchers have conducted a series of studies. As an important part of the seismic resistance in traditional wooden structures, the column rocking effect has drawn more and more attention recently.

Columns in traditional wooden structures are simply supported by cornerstones and are connected with beams by tenon joints (plug-slot type connection) [1]. When subjected to horizontal ground motion excitations, such columns can rock from side to side. Characteristics of the column rocking were clarified through theoretical and experimental studies, while its dynamic behavior for negative stiffness was investigated through parametric response analysis [2]. The energy conversion mechanism was tested on a full-scale timber structure model, finding that the gravitational potential energy due to column rocking is more than half of the energy input in the case of large cyclic amplitudes [3]. Discontinuous columns were typically used in traditional multi-story timber pagodas, and the rocking effect on seismic response of these pagodas was studied [4].

Instead of rocking columns, base rocking frames are generally adopted in steel structures to reduce and control unrepairable damages caused by earthquakes [5]. These base rocking frames only set a single rocking interface at their bases, which can be easily affected by the higher modes for high-rise buildings. The participation of higher modes contributes to the increase of member force in rocking frames, and thus limits the economic viability of rocking structural systems [6]. An effective solution to the limitation is to increase the number of rocking interfaces in the vertical direction of taller rocking systems [7]. This might also be a reasonable explanation for the discontinuity of columns in traditional multi-story timber pagodas. However, few studies discussed the application of rocking columns in steel structures, much less did they verify the mitigation of higher mode effects for multi-story steel structures equipped with rocking columns.

This paper proposes a multiple rocking steel frame system, also termed as rocking column system. In order to investigate the mechanism of the proposed system, the dynamic equation of motion of a single–story rocking column system (SRCS) was established. The difference of equations of motion between the SRCS and a single-story conventional frame system (SCFS) was compared. In addition, small shaking table tests were conducted to observe the seismic performance of the SRCS and a multi-story rocking column system (MRCS).

2. Proposed rocking column system

The proposed system comprises continuous beams, columns with end plates and gap bolts connecting the beam flanges with column end plates, and allows the columns to uplift and rock within a limited rotation angle. Plane frames of a SRCS and a MRCS are shown in Fig. 1. If the ground is accelerating to the left, the frames will initially rock to the right [$\theta(t) > 0$], as the dashed lines show in the figure. Sliding between the columns and the rigid ground, or between the columns and beams are not permitted in the frames. Therefore, columns at the same level of the structure have the same rotation angle, and the continuous beams keep horizontal all the time. This is different from the system of stacked rocking blocks where the upper blocks might start to rock at inclined rocking interfaces as shown in Fig. 2 [8]. In comparison with the stacked blocks, the MRCS has better stability in some cases because rocking columns always rock from horizontal interfaces.

To prevent overturning, gap bolts rather than post-tensioned tendons are used in the proposed system, which avoids additional vertical loads to the columns. A conventional beam-through steel frame can be converted into a frame of the SRCS or the MRCS by releasing the bolts of the connections, and this will not increase the difficulty of construction. Once the gaps of the bolts are exceeded, columns are constrained and deform the same as those in a rigid-jointed frame, otherwise only rocking motion happens. For the SRCS, it switches between a free rocking column system and a rigid-jointed frame. For the MRCS, it switches among the free rocking column system, the rigid-jointed frame and the hybrid state of the former two.

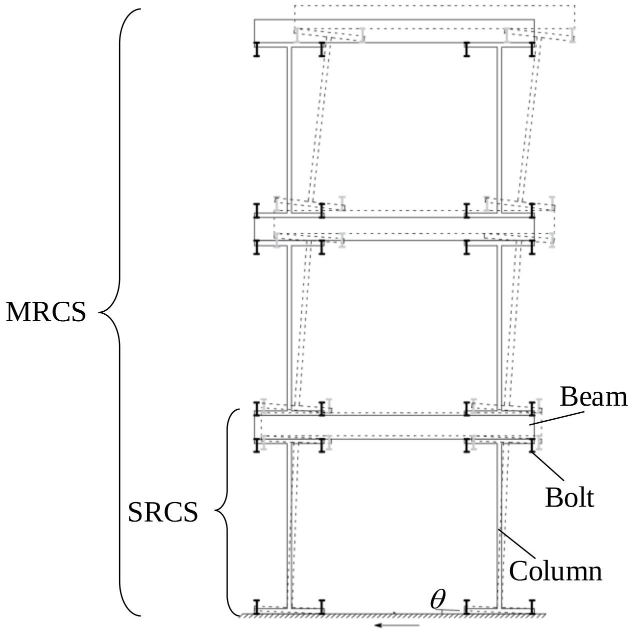

Fig. 1 – Schematic illustration of rocking column system

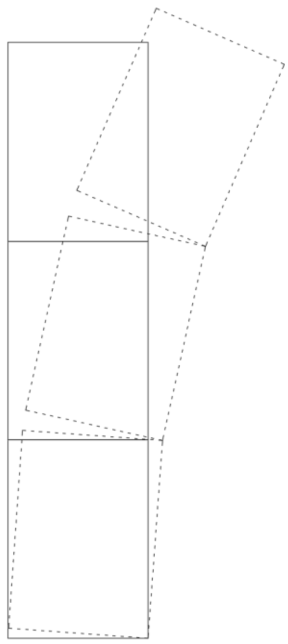

Fig. 2 – Three-rigid block system

3. Dynamic equation of motion

The analytical model of the SRCS is shown in Fig. 3, of which the height is $2h$ and the span is $2s$. Masses of the beam and column end plate, m_b and m_e, are supposed to be concentrated at their geometric centers, respectively, and mass of the column distributes uniformly with a linear density ρ. In this model, horizontal springs are used to simulate constraints for horizontal sliding between the beam and the column on each side. The beam and columns of the frame are assumed as rigid bodies in the analytical model, and the bolts are represented by vertical springs in the figure.

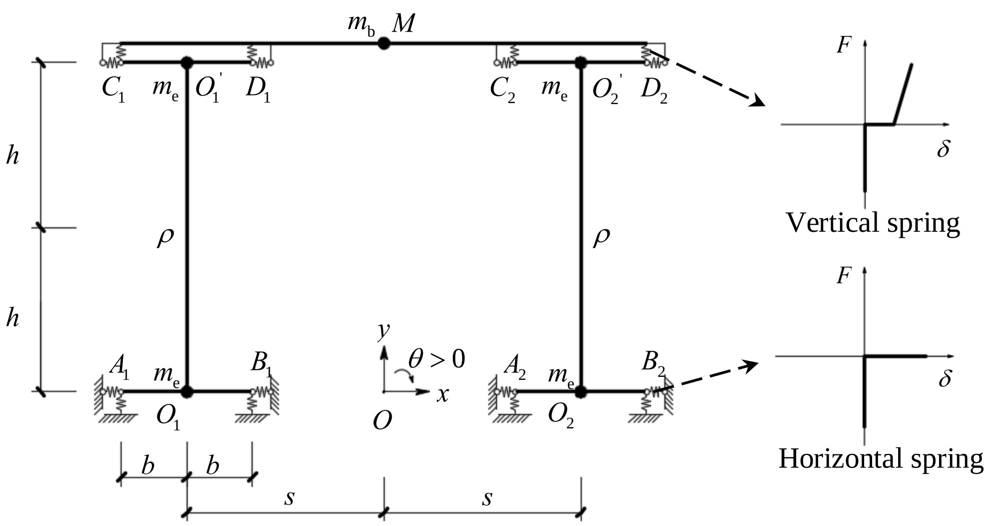

Fig. 3 – Analytical model of a single-story rocking column system

Assuming that the SCFS has the same size and mass with the SRCS in Fig. 3 and the structural damping is negligible, the equation of motion of the linear elastic SCFS can be obtained as

$$M_0\left(\ddot{x}_1+a_g\right)+K_0x_1=0 \tag{1}$$

$$M_0=m_b+2m_e+2\rho h \tag{2}$$

where the lumped mass, M_0, is the sum of the mass of the beam and the half mass of the columns with end plates, and K_0 is the lateral stiffness of the columns. a_g, $\ddot{x}_1+a_g$, $\ddot{x}_1$ and x_1 represent ground motion accleration, horizontal absolute acceleration, relative acceleration and displacement of the lumped mass in the SCFS.

As mentioned before, the SRCS will vibrate as the SCFS once the gap of the bolts are exceeded. In this state, the equation of motion of the SRCS can be written as

$$M_0\left(\ddot{x}_2+a_g\right)+K_0\left(x_2-d_{\lim}\right)=0 \tag{3}$$

$$d_{\lim}\approx 2h\theta_{\lim} \tag{4}$$

where $\ddot{x}_2+a_g$, $\ddot{x}_2$ and x_2 represent horizontal absolute acceleration, relative acceleration and displacement of the beam in the SRCS. $d_{\lim}$ is the limit inter-story drift of the beam when the rotation angle of the system reaches its limit value of $\theta_{\lim}$.

The equation of motion of the SRCS during rocking can be derived from Lagrange equation and obtained as

$$\begin{aligned}&2\left[\rho h(b^2+\tfrac{4}{3}h^2)+m_e(b^2+2h^2)+m_b(b^2+h^2)\right]\ddot{\theta}+g\left[\operatorname{sgn}(\theta)b\cos\theta-h\sin\theta\right](2\rho h+2m_e+m_b)\\&=-a_g(2\rho h+2m_e+m_b)\left[\operatorname{sgn}(\theta)b\sin\theta+h\cos\theta\right]\end{aligned} \tag{5}$$

Since $\theta_{\lim}$ is about 1°, sinθ and cosθ can be, respectively, approximated by θ and 1. Substituting Eq. (2) and $I_0 = 2[\rho h(b^2+4h^2/3)+m_e(b^2+2h^2)+m_b(b^2+h^2)]$ into Eq. (5), Eq. (5) can be rewritten as

$$I_0\ddot{\theta}+M_0g\left[\operatorname{sgn}(\theta)b-h\theta\right]=-M_0a_g\left[\operatorname{sgn}(\theta)b\theta+h\right] \tag{6}$$

The value of h is usually much larger than that of b, and thus $(b/h)^2$ is negligible. The ratio of M_0 to I_0 can be written as

$$\begin{aligned}\frac{M_0}{I_0}&=\frac{2\rho h+2m_e+m_b}{2\left[\rho h(b^2+\frac{4}{3}h^2)+m_e(b^2+2h^2)+m_b(b^2+h^2)\right]}\\&=\frac{2\rho h+2m_e+m_b}{2h^2\left[\rho h(\frac{b^2}{h^2}+\frac{4}{3})+m_e(\frac{b^2}{h^2}+2)+m_b(\frac{b^2}{h^2}+1)\right]}\\&\approx\frac{1}{2h^2}\end{aligned} \tag{7}$$

Since θ is a small angle and b is much less than h, $b\theta$ can be omitted in Eq. (6). Substituting $\ddot{x}_2=2h\ddot{\theta}$, $x_2=2h\theta$ and Eq. (7) into Eq. (6), Eq. (6) becomes

$$M_0\left(\ddot{x}_2+a_g\right)+M_0g\frac{2\operatorname{sgn}(x_2)b-x_2}{2h}=0 \tag{8}$$

$-M_0(\ddot{x}_1 + a_g)$ and $-M_0(\ddot{x}_2 + a_g)$ can be approximately regarded as the inter-story shear force of the SCFS and the SRCS, respectively. According to Eqs. (1), (3) and (8), the relationships between the inter-story shear forces and drifts are depicted in Fig. 4(a). In reality, the SRCS behaves the same as the SCFS when the inertial force of the SRCS is not enough to rotate the columns. Therefore, the force-drift relationship of the SRCS is modified as shown in Fig. 4(b).

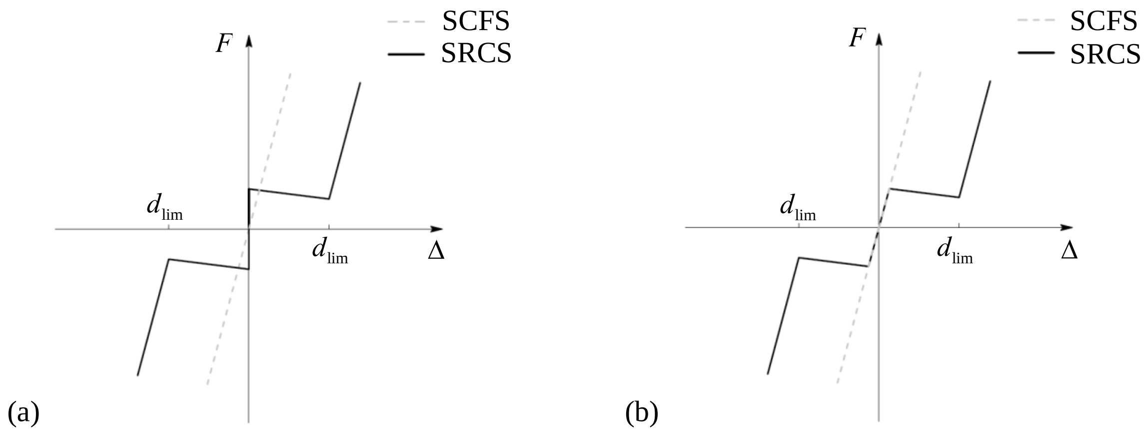

Fig. 4 – Force-drift curves of the SRCS: (a) Theoretical; (b) Modified

It can be observed from Fig. 4 that the SRCS is a highly nonlinear system. In Fig. 4(b), the stiffness curve of the SRCS can be divided into three parts, and the middle part has negative stiffness. The existence of negative stiffness could avert resonance of the system [9]. If the drift of the SRCS is less than $d_{\lim}$, the shear force of the SRCS could be smaller than that of the SCFS.

4. Small shaking table test

To investigate seismic performance of the proposed system, small shaking tests are conducted. The tested structures include the SRCS and the MRCS, and they can be respectively converted into the SCFS and the multi-story conventional frame system (MCFS) by screwing the bolts of the connections. The plan view of the structures is 240 mm×390 mm, and the height of each story is 313 mm. The mass and stiffness of the structures in the expected direction are designed to satisfy the fundamental periods of 0.1 s and 0.3 s for the SCFS and the MCFS. Ring beams with a height of 25 mm and a weight of 2 kg are rigid enough to substitute the floors of the frames. Columns with a size of 280 mm×30 mm×2 mm and end plates with a size of 240 mm×50 mm×4 mm are assembled together. According to Eq. (4), the value of $d_{\lim}$ in the tests is 5.76 mm when $\theta_{\lim}$ is designed to be 2.0%. Hemisphere shaped shear keys with a radius of 4 mm are used to prevent horizontal sliding between the beams and the column end plates.

Five ground motion records are selected from the PEER NGA (2016) database to cover a broad range of earthquake events. Peak ground accelerations (PGAs) of the ground motions are scaled to 0.07g, 0.20g and 0.40g, respectively, matching the PGAs of frequent earthquakes, design basis earthquakes and maximum considered earthquakes according to the Chinese Seismic Design Code.

Fourier spectra of the response histories of the SCFS and the SRCS under the same excitation of CAP000 of 0.07g are compared in Fig. 5. The dominant frequency of the SRCS is about 3.74 Hz, which is less than that of the SCFS, i.e., 9.80 Hz. It can be seen that the SRCS has smaller secant stiffness than the SCFS from Fig. 4.

For a comprehensive comparison of the performance of the SCFS and the SRCS, peak values of the inter-story shear forces and drifts of the structures under five excitations are given in Fig. 6. It can be observed that the inter-story shear forces of the SRCS are generally less than those of the SCFS when the drifts do not exceed d_{lim}. According to Eq. (8), the maximum shear force of the SRCS during rocking is 5.39 N, which is close to tested ones in the cases of the excitations FRN224, H05135, PSL180 and TMB205 of 0.07g. The maximum shear forces become much larger once the drifts are close to or larger than d_{lim}.

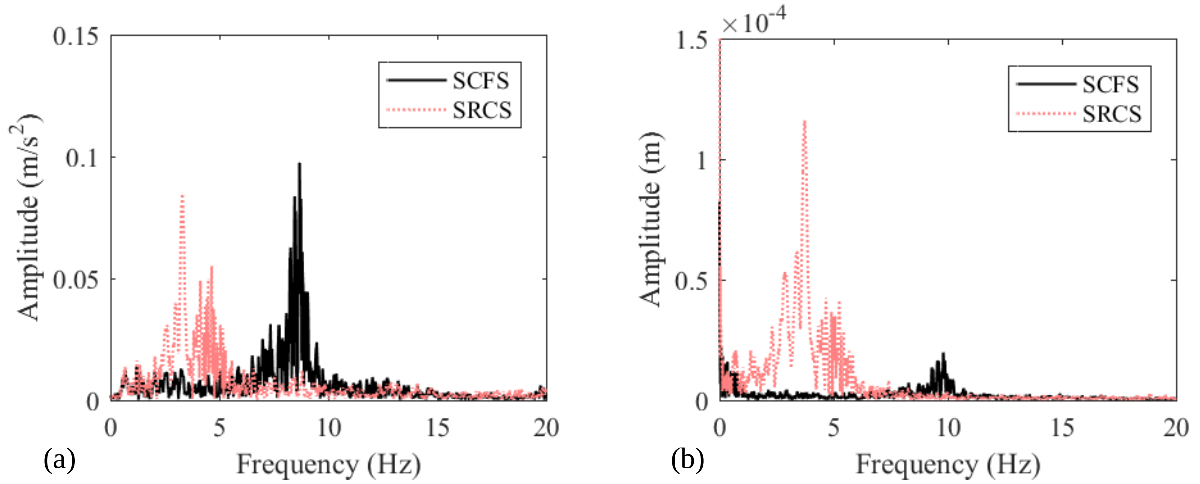

Fig. 5 – Fourier spectra of SCFS and SRCS under 0.07g scaled CAP000 input:
(a) Fourier spectrum of absolute acceleration; (b) Fourier spectrum of relative displacement

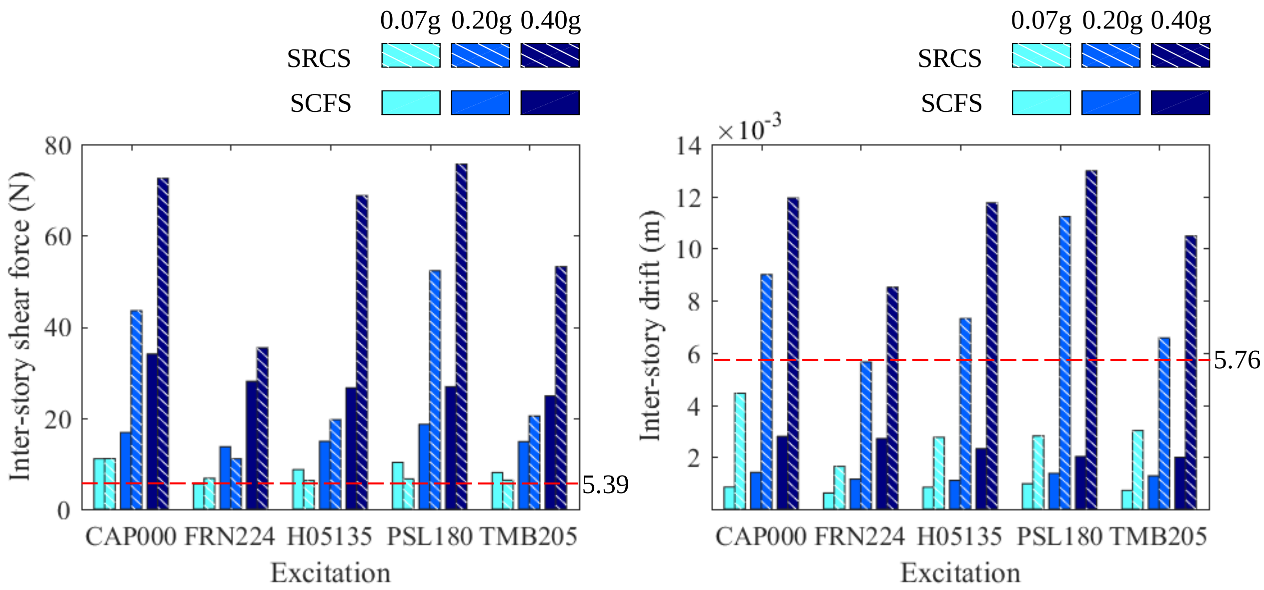

Fig. 6 – Response comparison of SCFS and SRCS:
(a) Peak values of inter-story shear forces; (b) Peak values of inter-story drifts

Based on the response time histories at the first level of the MCFS and the MRCS, the Fourier spectra of multi-story structures subjected to CAP000 of 0.07g are shown in Fig. 7 which indicates details of higher modes. The lowest dominant frequency of the MCFS is about 3.30 Hz, which is close to the designed value, 3.33 Hz. The tested frequencies regarding the second and third modes of the MCFS are 9.55 Hz and 13.70 Hz. The lowest dominant frequency of the MRCS is about 2.25 Hz, which is smaller than that of the MCFS. Some frequencies regarding higher modes of the MRCS can be seen in Fig. 7(b), whereas the values of those frequencies are different from those when the structure excited by different ground motions.

With respect to the multi-story structures, peak values of the inter-story shear forces and drifts at each level of the structures subjected to excitations of 0.07g are compared in Fig. 8. For most of the excitations, the shear forces of the MRCS are generally smaller than those of the MCFS, while it is reverse for the inter-story drifts. In the MCFS, both of the drifts and shear forces decrease from the first level to the third level. This is different from the MRCS, where the drifts increase while the shear forces decrease from the bottom to the top. In addition, it can be observed at the third level that the shear forces of the MRCS are larger than those of the MCFS if the drifts exceed d_{lim}, which is similar to the single-story structures.

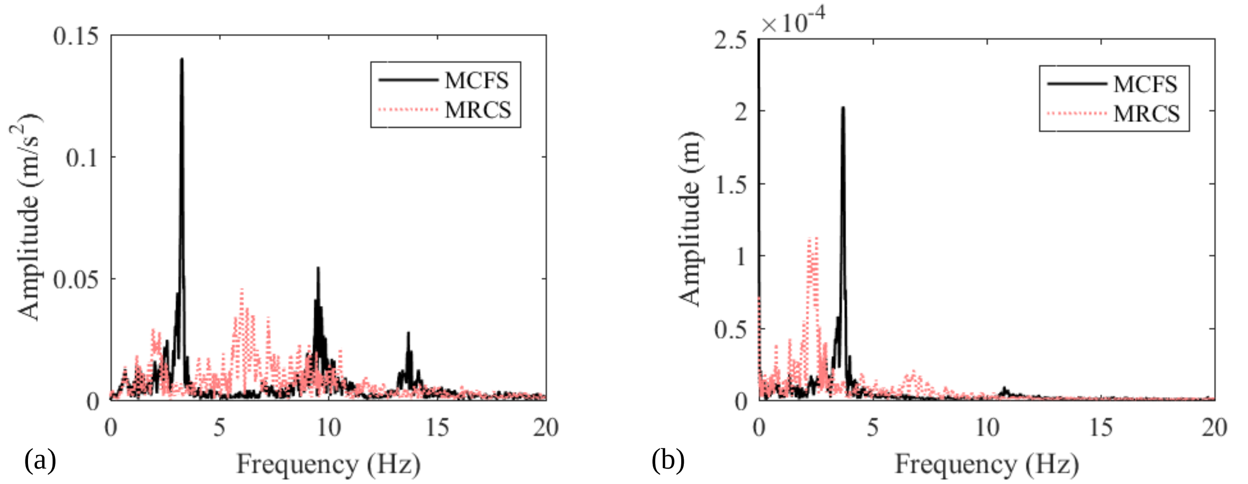

Fig. 7 – Fourier spectra of MCFS and MRCS under 0.07g scaled CAP000 input:
(a) Fourier spectrum of absolute acceleration; (b) Fourier spectrum of relative displacement

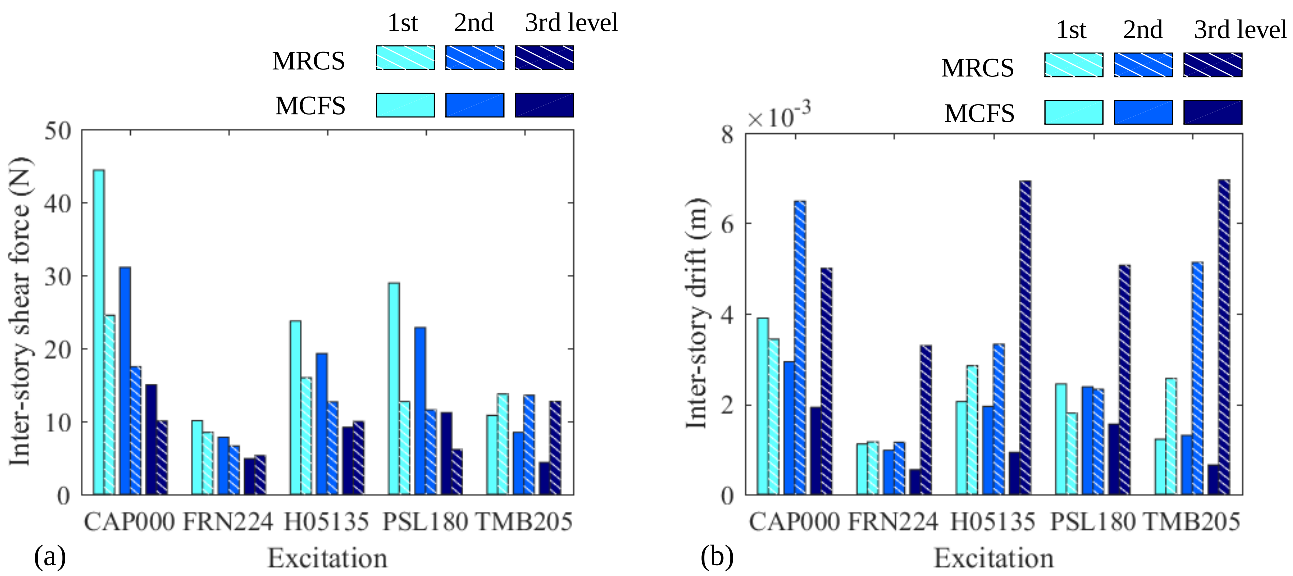

Fig. 8 – Response comparison of MCFS and MRCS under 0.07g scaled inputs:
(a) Peak values of inter-story shear forces at each level; (b) Peak values of inter-story drifts at each level

5. Conclusions

The proposed multiple rocking column system is a novel solution to the high mode effects in the base rocking structures. It can be realized by simply unscrewing the bolts of the connections between columns and beams, which allows the columns to rock and prevents potential overturning. The impacts during rocking motion dissipate seismic energy, and the gravity helps the structure to recenter. With the analytical and experimental studies, the main finding can be summarized as follows:

1) For the single-story rocking column system, if the columns are able to rock freely, the inter-story shear force can be reduced, and if not, the shear force increases dramatically.

2) Due to the existence of rocking motion, the secant stiffness of the single-story structure decreases, and so does the dominant frequency.

3) Frequencies of higher modes of the multi-story rocking column system vary with excitation inputs.

4) The multi-story rocking column system has smaller inter-story shear forces in most cases, and its inter-story drifts distribution is different from that of the conventional multi-story structure

6. Acknowledgements

This study is supported by National Nature Science Foundation of China (51978529). The authors gratefully acknowledge this support.

7. References

[1] Fang DP, Iwasaki S, Yu MH, Shen QP, Miyamoto Y, Hikosaka H (2001): Ancient Chinese timber architecture. I: Experimental study. *Journal of Structural Engineering*, **127** (11), 1348-1357.

[2] Maeda T (2008): Column rocking behavior of traditional wooden buildings in Japan. *10th World Conference on Timber Engineering*, Miyazaki, Japan.

[3] Meng X, Li T, Yang Q (2019): Experimental study on the seismic mechanism of a full-scale traditional Chinese timber structure. *Engineering Structures*, **180**, 484-493.

[4] Wu Y, Song X, Ventura C, Lam F (2019): Rocking effect on seismic response of a multi-story traditional timber pagoda model. *Engineering Structures*, 110009.

[5] Eatherton MR, Ma X, Krawinkler H, Mar D, Billington S, Hajjar JF, Deierlein GG (2014): Design concepts for controlled rocking of self-centering steel-braced frames. *Journal of Structural Engineering*, **140** (11), 04014082.

[6] Roke D, Sause R, Ricles JM, Gonner N (2009): Damage-free seismic resistant self-centering steel concentrically-braced frames. *Behaviour of Steel Structures in Seismic Areas*, Philadelphia, USA.

[7] Wiebe L, Christopoulos C, Tremblay R, Leclerc M (2013): Mechanisms to limit higher mode effects in a controlled rocking steel frame. 1: Concept, modelling, and low-amplitude shake table testing. *Earthquake Engineering & Structural Dynamics*, **42** (7), 1053-1068.

[8] Kounadis AN, Papadopoulos GJ (2016): On the rocking instability of a three-rigid block system under ground excitation. *Archive of Applied Mechanics*, **86** (5), 957-977.

[9] Makris N (2014): A half-century of rocking isolation. *Earthquakes and Structures*, **7** (6), 1187-1221.

